

# Large magnetoresistance of thick polymer devices having $\text{La}_{0.67}\text{Sr}_{0.33}\text{MnO}_3$ electrodes

A. Ozbay,<sup>1</sup> E. R. Nowak,<sup>1,a)</sup> Z. G. Yu,<sup>2</sup> W. Chu,<sup>2</sup> Yijian Shi,<sup>2</sup> S. Krishnamurthy,<sup>2</sup> Z. Tang,<sup>3</sup> and N. Newman<sup>3</sup>

<sup>1</sup>Department of Physics and Astronomy, University of Delaware, Newark, Delaware 19716, USA

<sup>2</sup>SRI International, Menlo Park, California 94025, USA

<sup>3</sup>School of Materials, Arizona State University, Tempe, Arizona 85287, USA

(Received 24 July 2009; accepted 14 November 2009; published online 9 December 2009)

We report magnetoresistance (MR) measurements for structures with micrometer-thick regioregular, polythiophene (rr-P3HT) polymer layers between two ferromagnetic contacts. Hole spin transport through the polymer layer leads to a relative MR value in 300 mT fields of 0.3% at 300 K and increasing to 18% at 25 K. The inferred intrinsic spin lifetime and diffusion length are about 7 ms and 0.4  $\mu\text{m}$ , respectively. The spin transport coherence length is enhanced by the electric field, leading to an enhancement in MR with increasing applied voltage. © 2009 American Institute of Physics. [doi:10.1063/1.3271772]

Being made of light atoms, organic semiconductors (OSCs) have very small spin-orbit coupling. Hence, they offer significant advantages for preserving spin coherence over longer times, and possibly longer distances, than in metallic or inorganic semiconducting layers. A focus of recent research has been to incorporate OSCs into spin-based electronics.<sup>1</sup>

Numerous studies have been made using OSC molecules, such as  $\text{Alq}_3$ , in both lateral<sup>2</sup> and vertical<sup>3</sup> spin valve (SV) structures, where carrier transport through the OSC ranges from tunneling to diffusive. Magnetoresistance (MR) ratios of  $\sim 10\%$  have been observed at low temperature ( $T$ ) but the MR decreases rapidly with  $T$  and is generally  $\leq 1\%$  at 300 K.<sup>1</sup> The majority of SV studies on thicker ( $\geq 10$  nm) layers of molecular-OSCs report widely varying MR values and spin diffusion lengths, and even reach conflicting conclusions.<sup>4</sup> There are only a few spin transport studies with high molecular weight polymers (such as BTQBT, P3OT, and rr-P3HT) and  $\text{La}_{0.67}\text{Sr}_{0.33}\text{MnO}_3$  (LSMO) electrodes.<sup>5-10</sup> Large MR was observed at low  $T$  but only 1.5% at 300 K in 100 nm thick rr-P3HT based SVs.<sup>9</sup>

There are no reports of substantial MR in spin-electronic devices having OSC spacer thicknesses significantly greater than 100 nm. Here, we report large MR measured in devices having a *micron or thicker* layer of the polymer, rr-P3HT. The spin diffusion length and relaxation lifetimes inferred from the MR data are on the order of 0.5  $\mu\text{m}$  and 1 ms, respectively, at low  $T$ . We further show that the observed MR increases with bias voltage, indicating that spin transport coherence length can be enhanced with electric field, in qualitative agreement with previous<sup>11,12</sup> and recent<sup>13</sup> predictions.

We have studied both lateral and vertical device geometries with the polymer rr-P3HT (Sigma-Aldrich, MW = 30 000). In our devices, holes are injected from a 300 nm thick film of LSMO grown on a  $\text{SrTiO}_3$  substrate. The pulsed laser deposited LSMO exhibits a Curie temperature  $T_C \sim 360$  K, a metal insulator transition at  $\sim 380$  K, and a resistivity  $\rho$  of 3.5  $\text{m}\Omega\text{cm}$  at room temperature and 0.3  $\text{m}\Omega\text{cm}$  at 20 K. In the vertical device, the top ferromagnetic (FM) Co electrode is thermally evaporated on the poly-

mer. The lateral devices were made by cutting (with ion beam milling) a 1  $\mu\text{m}$  wide trench in LSMO lines having a 300 nm thick  $\text{SiO}_x$  capping layer deposited by chemical-vapor-deposition (CVD). In these devices, both FM contacts are LSMO as depicted in the inset of Fig. 1. Each line is approximately 9  $\mu\text{m}$  long and the middle section of each line is 500  $\mu\text{m}$  wide. The coercive fields of the electrodes are nominally identical and our device is not a traditional SV device. Resistance measurements confirmed no conducting path existed either between lines or across the trench. The trench width, as shown in Fig. 1, varies from  $\sim 0.9$   $\mu\text{m}$  at the substrate to 1.5  $\mu\text{m}$  wide at the LSMO top surface. The trench was then back-filled with rr-P3HT by repeating several iterations of drop casting a 1 mg/100 mL P3HT-chloroform solution, sonication, and annealing at 100 °C for 30 min in a nitrogen gas atmosphere. No encapsulation was applied after annealing. The CVD-oxide on the top LSMO surface ensures the current path is only through the side walls. The current-voltage ( $I$ - $V$ ) characteristic of each line was measured multiple times between  $-5$  to  $+5$  V. If the  $I$ - $V$  was unstable (e.g., drifting), then the device was annealed again. Devices with negligible resistance drift were selected for further study. Measurements at room temperature were usually performed in air under ambient conditions and, for the case of low temperatures, in a He atmosphere.

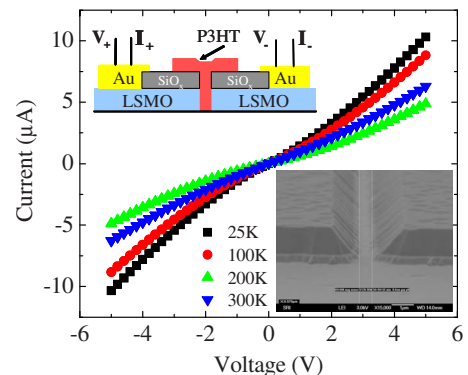


FIG. 1. (Color online) Temperature dependence of the  $I$ - $V$  curves for a lateral P3HT polymer device depicted in the inset. The SEM micrograph shows the trench sidewall profile.

<sup>a)</sup>Electronic mail: nowak@udel.edu.

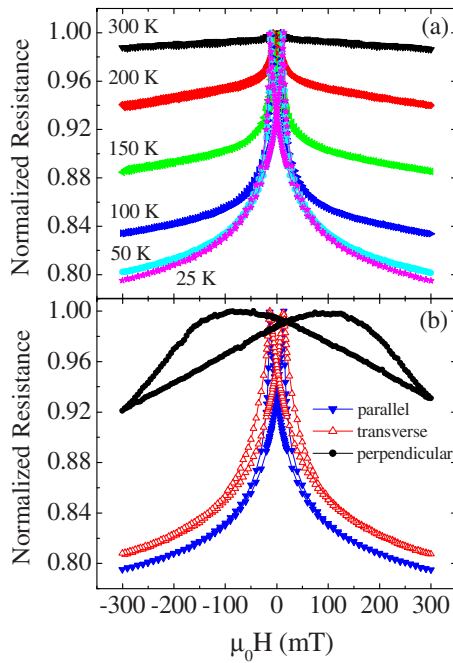


FIG. 2. (Color online) MR as a function of temperature (a) and for different orientations of the applied field at 25 K (b). The MR is normalized to its maximum value.

Ambient lighting had no discernable effect on the reported electrical properties.

We focus here on the MR properties of lateral devices. Figure 1 shows typical  $I$ - $V$  curves measured at several temperatures. The resistance was found to be a nonmonotonic function of temperature, exhibiting a maximum at roughly 200 K and a local minimum around 30 K. In the vertical device (not shown), the resistance also first increases with decreasing  $T$ , and then becomes roughly temperature independent below 100 K. Nonlinear  $I$ - $V$ s were a common feature of all devices and at all temperatures. Although the nonlinearity could arise from Schottky barriers at the interfaces, the measured current and its temperature dependence indicate that the polymer resistance determines the transport. Mechanisms such as a temperature and electric field dependent mobility, phonon scattering, trap filling, and space charge limited transport in the polymer could be responsible for the nonlinear transport.

Figure 2(a) shows the normalized MR,  $R(H)/R_{\max}$  ( $R_{\max}$  is the maximum resistance), at various temperatures. The MR was measured at a constant-voltage (3 V) bias with the magnetic field,  $H$ , applied parallel to the LSMO lines. All devices showed negative MR with  $R(H)$  decreasing at high fields. The resistance change increases with decreasing temperature and exceeds 20% at low  $T$ . The  $R(H)$  curves exhibit peaks that are somewhat symmetric about  $H=0$ . Figure 3(a) plots the temperature dependences of these fields together with the coercive field of the LSMO. Clearly, there exists a strong correspondence, indicating that the resistance peaks are due to the electrode magnetization and spin transport. Further evidence to support this claim is shown in Fig. 2(b), where  $H$  is applied either in-plane or out of plane. The MR exhibits similar field dependences for in-plane fields, either parallel or transverse to the LSMO electrodes, but it is considerably smaller and the resistance peaks are significantly more separated for case of perpendicular fields. The latter is expected since it is energetically unfavorable to pull the

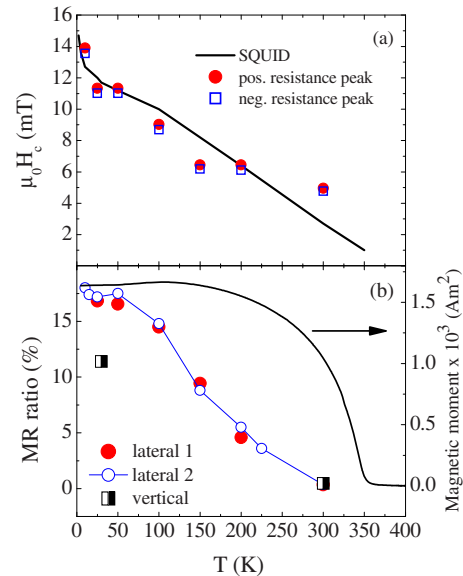


FIG. 3. (Color online) Temperature dependence of (a) the coercive field in LSMO and the fields at which the MR peaks occur and (b) of the LSMO magnetization and the MR ratio of three devices. The coercive field data and the magnetization curve are for an unpatterned LSMO film measured by SQUID magnetometry. MR was determined at 100 mT and using a 3 V bias.

magnetization out of the plane. This behavior establishes that the MR is related to the magnetization of the LSMO electrodes and that the increased magnetization of the contact increases the spin injection/collection efficiency, resulting in decreased resistance with increasing  $H$ . The MR can occur if the surface magnetizations of the LSMO sidewalls that form the trench are not well aligned at low fields. This is plausible given that SEM micrographs (Fig. 1 inset) show sidewall roughness resulting from the ion beam etching process. Such disorder alters the surface magnetic properties<sup>14</sup> and leads to different coercive fields for the magnetization in the two sidewalls and less abrupt switching of their magnetizations.

Other possible mechanisms for the observed MR include the following: anisotropic, organic, and colossal-magnetoresistance (AMR,<sup>15</sup> OMAR,<sup>16</sup> and CMR,<sup>17</sup> respectively). The large magnitude of the MR rules out AMR. We rule out OMAR because (1) no MR is observed in a vertical control device in which both magnetic electrodes were replaced by gold and (2) the MR exhibits dependence on field orientation [Fig. 2(b)]. CMR in the LSMO electrodes is also excluded because  $\rho_{\text{LSMO}}$  decreases by a factor of 11 when  $T$  is reduced from 300 to 25 K, whereas the change in normalized MR at 300 mT has increased by a factor of 10.

Figure 3(b) shows the temperature dependence of the MR ratio defined as  $|R(100 \text{ mT}) - R_{\max}|/R_{\max}$ . After correcting for the contribution from the LSMO electrodes, the MR ratio is approximately 0.3% at 300 K. The MR ratio increases with decreasing temperature, reaching about 18% at low  $T$ . Lower MR is observed in the vertical device as expected because of smaller spin polarization in Co. For comparison, Fig. 3(b) also shows the magnetization,  $M(T)$ , of the unpatterned LSMO film. The MR ratio begins to drop sooner and more rapidly with temperature than  $M(T)$ . Such behavior is common among organic SVs and is attributed to either a pronounced temperature dependence of the surface spin polarization at the electrode/OSC interface or a temperature dependent spin relaxation time.<sup>18</sup> Also, the LSMO sidewalls may have a reduced  $T_c$  due to the wall roughness. Although

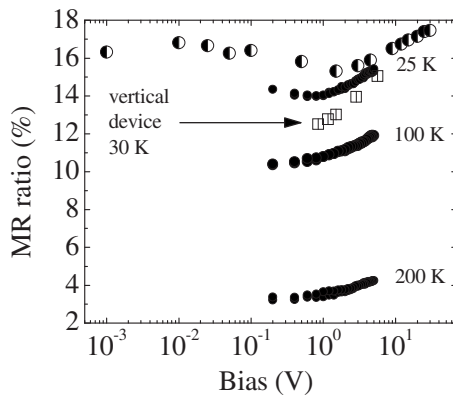


FIG. 4. Voltage bias dependence of the MR ratio determined at 300 mT for various temperatures. Solid circles represent data on the lateral device measured using a parallel applied field. Half-open circles are also for the lateral device but using a transverse field. Squares show data for the vertical device determined at 150 mT.

the surface quality of LSMO can be recovered through a vacuum thermal annealing treatment,<sup>19</sup> our attempts were unsuccessful, perhaps due in part to the different coefficients of thermal expansion between the CVD oxide and LSMO.

The MR ratio in our devices was found to be bias dependent. The bias dependence was determined by measuring the  $I$ - $V$  curves in 0 and 300 mT parallel fields and computed using the expression,  $|R(300 \text{ mT}) - R(0)|/R(0)$ . Figure 4 shows that the MR ratio in our devices increases with bias. This behavior is opposite to what is observed in OSC-based magnetic tunnel junctions<sup>1</sup> but qualitatively consistent with predictions by Yu *et al.*<sup>12</sup> The increase is most evident at low  $T$ ; while a change was not observed at 300 K. At 25 K, we also determined the MR ratio from  $R(H)$  sweeps measured at different bias voltages in transverse fields up to 300 mT. This data is shown by the half-open circles in Fig. 4. In this case, the range of bias voltages is greater and shows that the MR ratio is not monotonic, exhibiting a minimum near 1 V. The 30 K data plotted for the vertical device also shows MR increasing with bias.

The OSC layer in our devices is too thick for tunneling and its low mobility suggests that charge transport is through a highly diffusive hopping process. The spin diffusion length in P3HT can be crudely estimated using the modified Julliere relation,<sup>3,20</sup>  $\Delta R/R = 2P_1P_2 \exp[-d/\lambda_s]/(1 - P_1P_2 \exp[-d/\lambda_s])$ , where  $P_1$  and  $P_2$  are the spin polarizations of the electrodes,  $d$  is the OSC layer length, and  $\lambda_s$  is the spin diffusion length. However, this relation neglects the effect of electric field,  $E$ .  $\lambda_s$  should be regarded as the downstream spin diffusion length, which is  $\mu E \tau_s$  under high electric fields and  $(\mu k_B T \tau_s / e)^{1/2}$  at low fields.<sup>11,12</sup>  $\tau_s$  is the intrinsic spin relaxation time and the other quantities have their usual meaning. The low-field regime is defined as  $E < k_B T / e \lambda_s$  ( $\approx 50 \text{ V/cm}$ ) and is obtained in our devices with  $d = 1 \text{ }\mu\text{m}$  and bias voltages less than 5 mV. The Julliere relation, which can be used at low biases, yields a value of 380 nm for  $\lambda_s$  and using  $d = 1 \text{ }\mu\text{m}$ ,  $\Delta R/R \approx 16\%$  at 25 K and at 1 mV bias. We assumed  $P_1 = P_2 = 1$  because the efficient spin injection in spite of the conductivity mismatch between LSMO and the polymer indicates high spin polarization at the contacts.<sup>21</sup>

The mobility of P3HT is known to vary with morphology and processing conditions<sup>6,22,23</sup> and could not be measured once deposited in our devices. The value is typically

in the range between  $10^{-6}$  and  $10^{-2} \text{ cm}^2/\text{Vs}$  and  $\mu \approx 10^{-4} \text{ cm}^2/\text{Vs}$  explains the measured device resistance. For this value of  $\mu$ ,  $\tau_s$  is estimated to be 7 ms at low fields and low  $T$ . For  $\mu = 10^{-6} \text{ cm}^2/\text{Vs}$ ,  $\tau_s$  increases to 700 ms, and is comparable to the long spin relaxation times ( $\approx 1 \text{ s}$ ) reported by Pramanik *et al.*<sup>24</sup> for very low mobility Alq<sub>3</sub>. Nevertheless, the Julliere formula is inadequate to describe driven spin transport and the deduced value should be considered only as an estimate.

High carrier mobility may be an important factor for achieving very long spin transport coherence lengths in OSC compounds.<sup>25</sup> The mobility in organics is strongly field dependent and follows the Poole-Frenkel law. The field dependence becomes weaker in a system with high carrier density,<sup>26</sup> as in the present case. This can lead, through a reduction in transit time across the polymer, to an enhancement in MR with increasing bias such as we observe. Our studies indicate that spin transport distances in excess of microns can be attained in relatively low-mobility polymers. However, the low yield of stable devices in our studies and the widely varying MR ratios reported by others<sup>5,6,8-10</sup> in vertical SV structures highlight the need for detailed investigations aimed at understanding the chemical, structural, and morphological properties that influence spin transport in organic materials.

This work was supported by ONR under Contract No. N00014-07-C-0393. E.R.N. also acknowledges partial support by DOE under Award No. DE-FG02-07ER46374 and thanks G. Szulczewski for many stimulating discussions.

<sup>1</sup>W. J. M. Naber, S. Faez, and W. G. van der Wiel, *J. Phys. D* **40**, R205 (2007).

<sup>2</sup>V. Dediu, M. Murgia, F. C. Matocotta, C. Taliani, and S. Barbanera, *Solid State Commun.* **122**, 181 (2002).

<sup>3</sup>Z. H. Xiong, D. Wu, Z. Valy Vardeny, and J. Shi, *Nature (London)* **427**, 821 (2004).

<sup>4</sup>J. S. Jiang, J. E. Pearson, and S. D. Bader, *Phys. Rev. B* **77**, 035303 (2008).

<sup>5</sup>D. Dhandapani *et al.*, *IEEE Trans. Magn.* **44**, 2670 (2008).

<sup>6</sup>D. Dhandapani *et al.*, *J. Appl. Phys.* **105**, 07C702 (2009).

<sup>7</sup>T. Ikegami *et al.*, *Appl. Phys. Lett.* **92**, 153304 (2008).

<sup>8</sup>J. Kumar *et al.*, *Solid State Commun.* **138**, 422 (2006).

<sup>9</sup>S. Majumdar, R. Laiho, P. Laukkanen, I. J. Vayrynen, H. S. Majumdar, and R. Osterbacka, *Appl. Phys. Lett.* **89**, 122114 (2006).

<sup>10</sup>N. A. Morley *et al.*, *J. Appl. Phys.* **103**, 07F306 (2008).

<sup>11</sup>Z. G. Yu, M. A. Berding, and S. Krishnamurthy, *Phys. Rev. B* **71**, 060408 (2005).

<sup>12</sup>Z. G. Yu and M. E. Flatte, *Phys. Rev. B* **66**, 235302 (2002).

<sup>13</sup>P. A. Bobbert, W. Wagemans, F. W. A. van Oost, B. Koopmans, and M. Wohlgenannt, *Phys. Rev. Lett.* **102**, 156604 (2009).

<sup>14</sup>J. H. Park *et al.*, *Phys. Rev. Lett.* **81**, 1953 (1998).

<sup>15</sup>R. C. O'Handley, *Modern Magnetic Materials: Principles and Applications* (Wiley, New York, 2000).

<sup>16</sup>O. Mermer *et al.*, *Phys. Rev. B* **72**, 205202 (2005).

<sup>17</sup>M. B. Salamon and M. Jaime, *Rev. Mod. Phys.* **73**, 583 (2001).

<sup>18</sup>F. J. Wang and Z. Valy Vardeny, *J. Mater. Chem.* **19**, 1685 (2009).

<sup>19</sup>M. P. de Jong, V. A. Dediu, C. Taliani, and W. R. Salaneck, *J. Appl. Phys.* **94**, 7292 (2003).

<sup>20</sup>M. Julliere, *Phys. Lett. A* **54**, 225 (1975).

<sup>21</sup>G. Schmidt, D. Ferrand, L. W. Molenkamp, A. T. Filip, and B. J. van Wees, *Phys. Rev. B* **62**, R4790 (2000).

<sup>22</sup>J.-F. Chang *et al.*, *Chem. Mater.* **16**, 4772 (2004).

<sup>23</sup>L. A. Majewski, J. W. Kingsley, C. Balocco, and A. M. Song, *Appl. Phys. Lett.* **88**, 222108 (2006).

<sup>24</sup>S. Pramanik *et al.*, *Nat. Nanotechnol.* **2**, 216 (2007).

<sup>25</sup>J. H. Shim *et al.*, *Phys. Rev. Lett.* **100**, 226603 (2008).

<sup>26</sup>Z. G. Yu, D. L. Smith, A. Saxena, R. L. Martin, and A. R. Bishop, *Phys. Rev. B* **63**, 085202 (2001).